Second-harmonic-generation rings and refractive-index measurement in uniaxial crystals

Rick Trebino

Noncollinear second-harmonic-generation (SHG) processes involving an unfocused laser beam and its scattered radiation can act to produce one or more cones of phase-matched second harmonic, resulting in rings on an observation screen. We calculate expressions for the ring parameters (center and radius) for types I and II uniaxial crystals in terms of the crystal indices of refraction and geometry. Measurement of the ring parameters for several crystal tilt angles can yield very accurate relative values for the indices of refraction of a uniaxial SHG crystal. A method for the automatic maintenance of optimum SHG which does not require the placement of optics in the beam is also suggested.

I. Introduction

In addition to the well-known collinear phase-matching directions in nonlinear optical crystals, there can be in general a wide range of phase-matched noncollinear second-harmonic-generation (SHG) processes for arbitrary propagation directions in the same crystals.[1,2] Such processes can involve the **k** vector of the main (unfocused) fundamental beam mixing vectorially with a (scattered) off-axis fundamental wave to yield, in a phase-matched manner, a relatively strong second-harmonic wave. Many scattered wave directions yielding phase-matched SHG usually exist, giving rise to interesting ring-shaped patterns near the spot of the main beam on an observation screen. For example, in type II SHG, as many as three off-center rings can be observed around the main beam spot. Observation and correct interpretation of these rings were first reported by Giordmaine who treated only the special case of a negatively birefringent type I crystal and hence observed only one ring.[3]

When the main laser beam propagates within a few degrees of, but not exactly in, the direction required for collinear phase-matching, these rings can be as bright as or even brighter than the unphase-matched second-harmonic spot produced by the main beam, even in high quality crystals in which very little scattering occurs. Consider that

$$P(2\omega_0) = \eta P_1(\omega_0) P_2(\omega_0), \tag{1}$$

where η is the second-harmonic-power-generation efficiency. For the unphase-matched collinear interaction, $P_1(\omega_0)$ and $P_2(\omega_0)$ are large, but η is very small. For phase-matched noncollinear processes involving one **k** vector contributed by the main beam plus one scattered low intensity **k** vector, $P_1(\omega_0)$ and η will be large, but $P_2(\omega_0)$ will be small yielding, conceivably, a comparable $P(2\omega_0)$.

This note details an examination of these processes in birefringent uniaxial crystals. A first-order analysis yields all the salient features of the phenomenon and indicates the off-center ringlike structure of the locus of phase-matched second-harmonic propagation directions. The angular radii of these rings provide a very sensitive measure of the phase-mismatch, implying that measurements of ring centers and radii may be used for extremely precise relative determinations of uniaxial SHG crystal indices of refraction. A second-order calculation is then done for use in such determinations. These results are also applicable to automatic alignment schemes for SHG optimization.

II. First-Order Calculations

Consider first a SHG crystal which has approximately zero birefringence ($n_e \approx n_o$) with $n(\omega_0) > n(2\omega_0)$. (This is somewhat unphysical but serves as a simple illustration.) Collinear phase-matching will not be possible, but an off-axis scheme for which $n(\omega_0)\cos\alpha = n(2\omega_0)$ will be phase-matched (see Fig. 1). Hence a cone of diverging second-harmonic radiation of angular radius

The author is with Stanford University, Edward L. Ginzton Laboratory, Stanford, California 94305.

Received 12 September 1980.
0003-6935/81/122090-07$00.50/0.

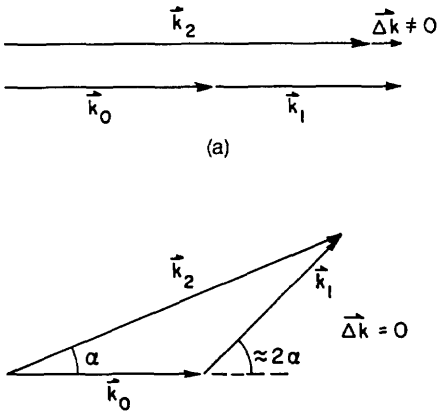

Fig. 1. $\mathbf{k}_0$ and $\mathbf{k}_1$ are fundamental beam $\mathbf{k}$ vectors. $\mathbf{k}_2$ is the second harmonic. (a) Collinear process is not phase-matched. (b) Noncollinear process in which $\mathbf{k}_0$ is the main laser beam, $\mathbf{k}_1$ is a scattered off-axis fundamental wave, and $\mathbf{k}_2$ is the phase-matched off-axis second-harmonic $\mathbf{k}$ vector.

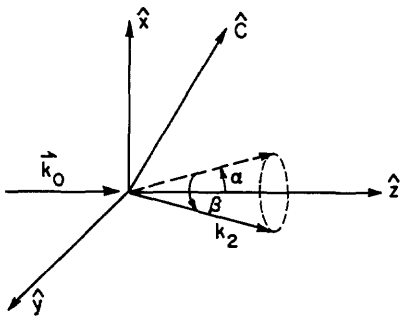

Fig. 2. Crystal and $\mathbf{k}$ vector geometry. $\hat{c}$ lies in the x-z plane at angle θ_0 to the z axis. Direction of $\mathbf{k}_2$ is obtained by rotating $\hat{z}$ by a small angle α about the y axis and then rotating the obtained vector further by an angle β about the z axis.

α will surround the main beam. The case $n(\omega_0) < n(2\omega_0)$ would require $\cos\alpha$ to be larger than unity, and hence no analogous solutions will exist.

Now consider a fundamental beam propagating with $\mathbf{k}$ vector

$$\mathbf{k}_0 = \frac{2\pi}{\lambda_0} n_i(\omega_0,\theta_0)\hat{z} \tag{2}$$

through a birefringent uniaxial crystal whose c axis is defined by the unit vector

$$\hat{c} = \cos\theta_0\hat{z} + \sin\theta_0\hat{x}, \tag{3}$$

where λ_0 is the fundamental wave free space wavelength, θ_0 is the propagation angle with respect to the c axis, and $n_i(\omega_0,\theta_0)$ is the (ordinary or extraordinary) index of refraction of the crystal at the above frequency and propagation direction. An off-axis second-harmonic $\mathbf{k}$ vector will be given by

$$\mathbf{k}_2 = \frac{2\pi}{\left(\frac{1}{2}\lambda_0\right)} n_k(2\omega_0,\theta_2)(\sin\alpha\cos\beta\hat{x} + \sin\alpha\sin\beta\hat{y} + \cos\alpha\hat{z}), \tag{4}$$

where α is the angle between $\mathbf{k}_0$ (or $\hat{z}$) and $\mathbf{k}_2$, β is the angle by which $\mathbf{k}_2$ is rotated about the z axis out of the x-z plane (see Fig. 2), $n_k(2\omega_0,\theta_2)$ is the index of refraction of this wave, and θ_2 is the angle between $\mathbf{k}_2$ and the c axis:

$$\cos\theta_2 = \frac{\mathbf{k}_2\cdot\hat{c}}{|\mathbf{k}_2||\hat{c}|}, \tag{5}$$

$$= \cos\theta_0\cos\alpha + \sin\theta_0\sin\alpha\cos\beta. \tag{6}$$

Referring to Fig. 1(b), the required scattered fundamental wave must propagate at an angle of approximately 2α to the fundamental in the plane of $\mathbf{k}_0$ and $\mathbf{k}_2$, so that its angle with respect to the c axis will be given by

$$\cos\theta_1 \approx \cos\theta_0\cos 2\alpha + \sin\theta_0\sin 2\alpha\cos\beta. \tag{7}$$

The approximate phase-matching condition (valid for type I or II SHG) is then

$$\frac{1}{2}[n_i(\omega_0,\theta_0) + n_j(\omega_0,\theta_1)]\cos\alpha = n_k(2\omega_0,\theta_2), \tag{8}$$

where $n_j(\omega_0,\theta_1)$ is the index of refraction of the scattered fundamental wave.

Each extraordinary index of refraction required in Eq. (8) can be approximated to first order in α about its value at $\theta = \theta_0$ using

$$n_e(\omega,\theta) = \{n_e^{-2}(\omega) - [n_e^{-2}(\omega) - n_o^{-2}(\omega)]\cos^2\theta\}^{-1/2} \tag{9}$$

for $\omega = \omega_0$ or $2\omega_0$, where $n_o(\omega)$ and $n_e(\omega)$ are the ordinary and extraordinary indices of refraction of the crystal at frequency ω, and θ is the angle of propagation with respect to the c axis. Second-order terms in α will be small relative to the $\frac{1}{2}\alpha^2$ term contributed by the $\cos\alpha$ factor in Eq. (8). The results for $n_e(\omega_0,\theta_1)$ and $n_e(2\omega_0,\theta_2)$ are

$$n_e(\omega_0,\theta_1) \approx n_e(\omega_0,\theta_0) + 2A_1\alpha\cos\beta, \tag{10}$$

$$n_e(2\omega_0,\theta_2) \approx n_e(2\omega_0,\theta_0) + A_2\alpha\cos\beta, \tag{11}$$

where

$$A_1 = A_1(\omega_0,\theta_0) = \frac{1}{2}b_1 n_e^3(\omega_0,\theta_0)\sin 2\theta_0, \tag{12}$$

$$A_2 = A_2(2\omega_0,\theta_0) = \frac{1}{2}b_2 n_e^3(2\omega_0,\theta_0)\sin 2\theta_0, \tag{13}$$

$$b_1 \equiv n_e^{-2}(\omega_0) - n_o^{-2}(\omega_0), \tag{14}$$

$$b_2 \equiv n_e^{-2}(2\omega_0) - n_o^{-2}(2\omega_0). \tag{15}$$

Clearly it is not necessary to expand $n_i(\omega_0,\theta_0)$, and all ordinary indices of refraction are independent of angle. In the following analysis, $n_j(\omega_0,\theta_0)$ and $n_k(2\omega_0,\theta_0)$ will always be expanded as in Eqs. (10) and (11), but it will be understood that A_l will vanish if the corresponding wave is ordinary.

Substitution of Eqs. (10) and (11) into the phase-matching condition [Eq. (8)], keeping the second-order term in α contributed by $\cos\alpha$ only, yields an equation of the form

$$\alpha^2 - 2\alpha\alpha_c\cos\beta + \alpha_c^2 - \alpha_R^2 = 0. \tag{16}$$

This is the equation for a cone of rays (a ring if viewed

on a screen, see Fig. 3) of angular radius α_R about a central angle α_c with respect to $\hat{z}$ in the x-z plane. (This central ray will be tilted toward the c axis if $\alpha_c > 0$ and away if $\alpha_c < 0$.) The ring center and radius will be

$$\alpha_c = (A_1 - A_2)/n, \tag{17}$$

$$\alpha_R = \sqrt{\left(\frac{A_1 - A_2}{n}\right)^2 + \frac{2\Delta n}{n}}, \tag{18}$$

where

$$n = \frac{1}{2}[n_i(\omega_0,\theta_0) + n_j(\omega_0,\theta_0)], \tag{19}$$

$$\Delta n = \frac{1}{2}[n_i(\omega_0,\theta_0) + n_j(\omega_0,\theta_0)] - n_k(2\omega_0,\theta_0). \tag{20}$$

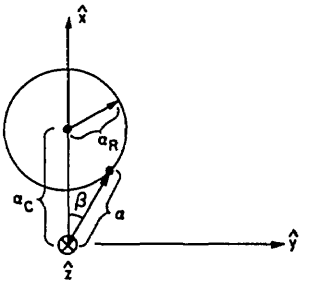

Fig. 3. Angular polar coordinates α and β and a cone of rays centered about a ray at an angle α_c from the z axis (toward the c axis) with angular radius α_R.

The quantity Δn is the index-mismatch of the collinear process. Note that for positive values of Δn, a ring will exist containing the main beam ($\mathbf{k}_0$); for $\Delta n = 0$ the collinear process will be phase-matched, but the resulting very intense spot is only part of a ring resulting from phase-matched not-necessarily-collinear processes; for $\Delta n < 0$ the ring will not contain the main beam, and for Δn sufficiently negative, the ring radius will approach zero, beyond which no ring appears. By smoothly varying the tilt angle of a crystal, this evolution of ring size and position is easily seen and may be used to attain and maintain index matching.

Table I. Noncollinear Phase-Matching Processes

	Type of Phase-matching	Polarization: Main Beam	Polarization: Scattered Fundamental	Polarization: Second Harmonic	Formulas for Ring Centers (α_c) and Ring Radii (α_R) (to first order)
(a)	I	0	0	E	$\alpha_c = \frac{-A_2}{n}$; $\alpha_R = \sqrt{\left(\frac{A_2}{n}\right)^2 + \frac{2\Delta n}{n}}$
(a)	II	0	E	E	$\alpha_c = \frac{A_1 - A_2}{n}$; $\alpha_R = \sqrt{\left(\frac{A_1 - A_2}{n}\right)^2 + \frac{2\Delta n}{n}}$
(a)	II	E	0	E	$\alpha_c = \frac{-A_2}{n}$; $\alpha_R = \sqrt{\left(\frac{A_2}{n}\right)^2 + \frac{2\Delta n}{n}}$
(b)	I	E	E	0	$\alpha_c = \frac{A_1}{n}$; $\alpha_R = \sqrt{\left(\frac{A_1}{n}\right)^2 + \frac{2\Delta n}{n}}$
(b)	II	0	E	0	$\alpha_c = \frac{A_1}{n}$; $\alpha_R = \sqrt{\left(\frac{A_1}{n}\right)^2 + \frac{2\Delta n}{n}}$
(b)	II	E	0	0	$\alpha_c = 0$; $\alpha_R = \sqrt{\frac{2\Delta n}{n}}$

Type II rings will exist if both fundamental polarizations are present and if sufficient birefringence for Type II phase-matching exists. Ring intensity will depend on the value of d_{eff} and the amount of scattered radiation present in the required directions.

(a) Processes in negatively birefringent crystals (e.g. CDA, KDP, $LiNbO_3$, $LiIO_3$);
(b) Processes in positively birefringent crystals (e.g., CdGeAs$_2$, CdSe).

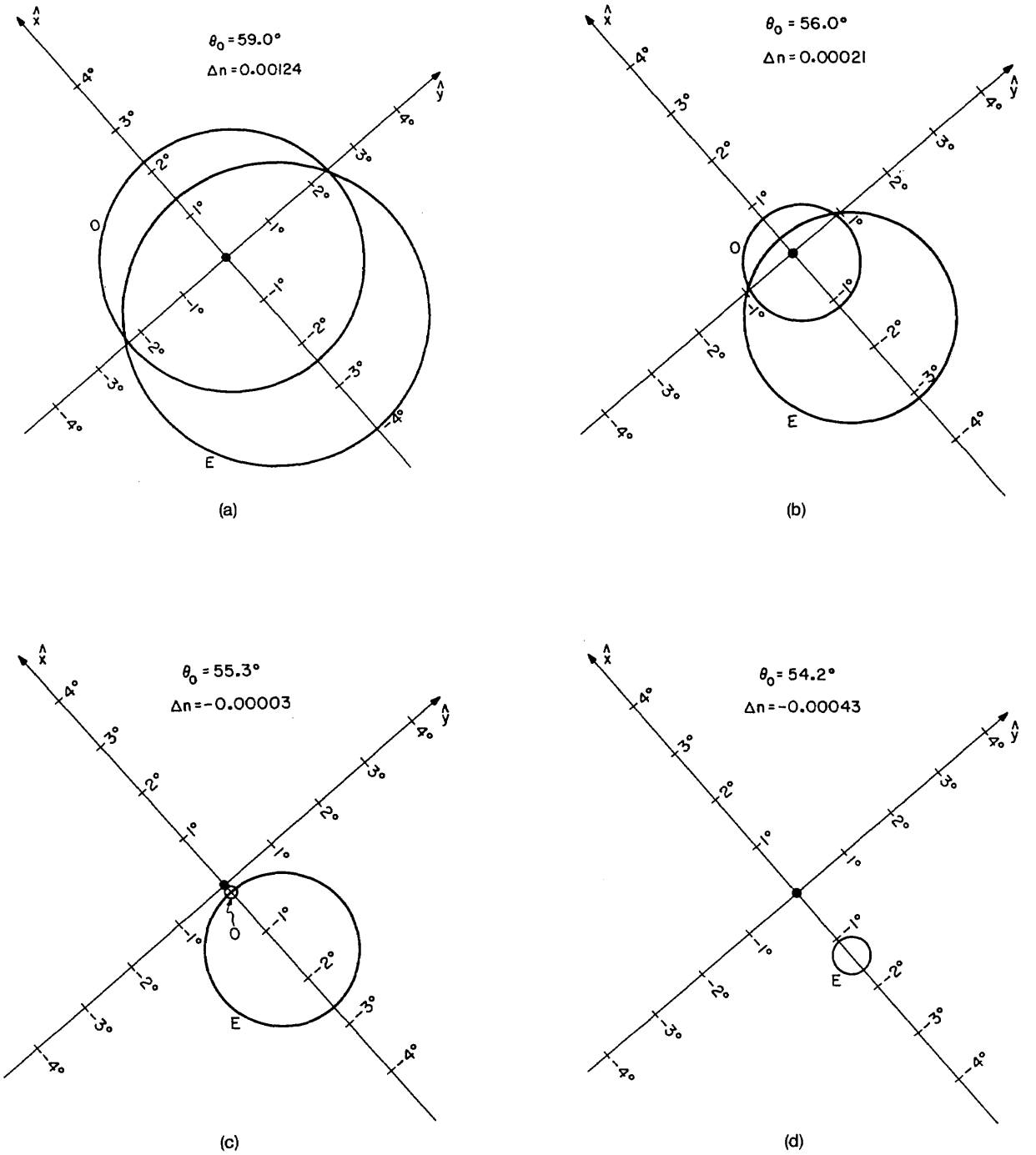

Fig. 4. Predicted ring patterns of the two type II (0.532-μm) rings obtained with 1.06-μm radiation in a type II KD*P crystal. The spot at the origin of each coordinate system corresponds to the unscattered laser beam. The crystal c axis intersects the x axis in each figure at the value θ_0. The calculated phase-matching angle is $\theta_0 = 55.4°$. (The index of refraction data used were taken from Ref. 4.) The polarization of the scattered light giving rise to each ring is indicated by E or 0: (a) $\Delta n \gg 0$; (b) $\Delta n > 0$; (c) Δn slightly less than 0; (d) $\Delta n < 0$.

For a type I SHG crystal with insufficient birefringence for type II phase-matching or for which only one polarization of fundamental radiation is present, a ring with the above characteristics will be observed. A far more interesting crystal, however, is a type II SHG crystal. For such a crystal, two type II processes exist, each giving rise to a separate ring, and, in addition, a type I process will produce an additional ring (see Table I). Thus for type II SHG crystals, three rings may be observed. The intensity of the type I ring will be dependent on the value of d_{eff} for the type I process responsible for it, which may be very low in a crystal optimized for type II SHG.

III. Comparison with Experiment

A CD*A crystal cut for type I 90° phase-matching of (ordinary) 1.06-μm radiation at a temperature of 106°C was employed at room temperature. Approximately 8 MW/cm^2 of highly collimated fundamental radiation with ordinary polarization propagating at an angle of 90° with respect to the c axis produced a 0.532-μm ring with extraordinary polarization which was centered (to within 0.05°) on the main beam with an angular radius (external to the crystal) of 2.5° ± 0.1°. For CD*A at room temperature, n_e (0.532 μm) = 1.5495 and n_o(1.06

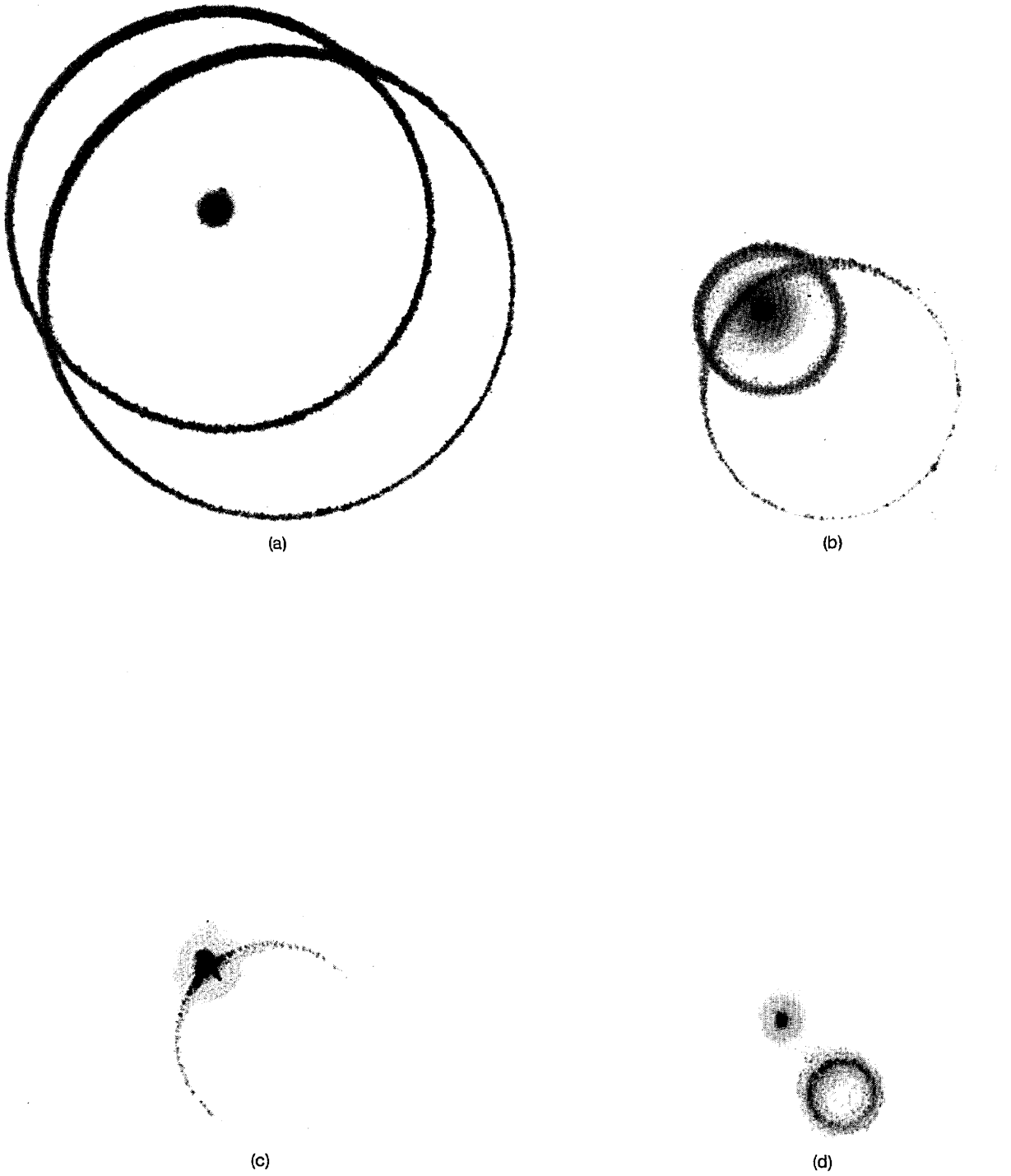

Fig. 5. Photographs of the two type II (0.532-μm) rings obtained with 1.06-μm radiation in a type II KD*P crystal. The spot in each figure is that of the unscattered laser beam. Values of the crystal tilt angles are approximately those in the corresponding figures of Fig. 4. The very small predicted ring in Fig. 4(c) is not evident in Fig. 5(c) probably because of obscuration by the larger ring and main beam spot. The type I ring in each case was larger than the camera frame and too dim to photograph.

μm) = 1.5503, and for the above geometry $A_1 = A_2 = 0$ so that $\alpha_c = 0°$, and, corrected for refraction at the crystal exit face, theory predicts $\alpha_R^{ext} = 2.52°$ in agreement with experiment.

A type II KD*P crystal was also studied at the above wavelengths, and all three predicted rings were observed. Near the phase-matching angle for collinear type II SHG, the type I ring is so severely phase-mismatched (Δn is large) that the ring radius is of the order of 7° (internal to the crystal), and, hence, it is difficult to observe because scattering this far off axis is very weak. Furthermore, d_{eff} for this ring is much smaller than that for the type II processes, and, as a result, the large type I ring was very dim. The theoretically expected type II rings are shown in Fig. 4, and photographs of the two type II rings showing their evolution (as a function of θ_0, the crystal tilt angle) are shown in Fig. 5. Qualitative agreement with the theoretically calculated rings is thus obtained.

IV. Application to Index of Refraction Measurement

The values of the ring parameters are extremely sensitive measures of the index-mismatch. When θ_0 is within 1° or so of the collinear phase-matching angle, the index-mismatch Δn is ~0.0003 or less. This means that using index of refraction data accurate to five digits (e.g., $n_e = 1.4588$), only one-digit accuracy is obtained in α_R [when the Δn term dominates in Eq. (18)—which is usually the case], which can be measured to as many as three digits. Thus it is possible that the expressions for the ring parameters (α_c and α_R for the one, two, or three rings observed) can be inverted to obtain expressions for the three or four relevant indices of refraction of a uniaxial SHG crystal, which could be very accurate.

Several considerations must be kept in mind, however, before attempting such a measurement. First, errors in the measured values of the ring radii result in much smaller errors in the derived values of the indices of refraction, while errors in the measured values of the ring centers are magnified. This can be seen by noting that, if n_l is one of the crystal indices of refraction, $\partial n_l/\partial \alpha_R \approx n\alpha_R \ll 1$, while $\partial n_l/\partial \alpha_c \gg 1$. Thus measured values of α_R only are useful for index of refraction determination. An experiment using this technique would then involve measurement of many values of α_R for different crystal tilt angles θ_0, yielding statistical data which may be curve-fit to obtain the required crystal parameters.

While the statistical nature of the above experiment implies even greater precision, the technique suffers from the fundamental limitation that only relative values of the indices of refraction are obtainable. For example, consider a type II positively birefringent crystal [for which $n_o(\omega_0)$, $n_e(\omega_0)$, and $n_o(2\omega_0)$ appear in the ring parameter expressions]. Equation (18) can be linearized by writing $n_l(\omega) = n_l^{(o)}(\omega) + \Delta n_l(\omega)$, where $n_l^{(o)}(\omega)$ is an approximate known value of $n_l(\omega)$, and $\Delta n_l(\omega)$ is small, so that only first-order terms in $\Delta n_o(\omega_0)$, $\Delta n_e(\omega_0)$, and $\Delta n_o(2\omega_0)$ must be retained. Two linearly independent equations may be obtained by measuring two ring radii, but three or more measurements yield dependent equations and only serve to better pin down ratios or differences of indices of refraction. Thus accurate absolute information is not available.

The relative information that can be obtained will be very accurate and, in some cases, very useful. The temperature dependence of the index mismatch can be obtained to great accuracy easily. Also knowledge of one of the indices of refraction at one frequency in an SHG process will generally be sufficient to provide all the remaining information.

Clearly, more precise expressions for the ring parameters than those given in the preceding largely physical argument will be necessary to achieve significant accuracy. Second-order terms in α must be included in all quantities, the value of θ_1 [previously given by Eq. (7)] must be improved, and Poynting vector walkoff must be considered. The next section presents a derivation of the ring parameters in which the above effects are included.

V. Second-Order Calculation

Writing $\mathbf{k}_1$ as that vector which satisfies the phase-matching condition exactly (i.e., $\mathbf{k}_1 = \mathbf{k}_2 - \mathbf{k}_0$) and using Eqs. (2)–(6), we find that

$$|\mathbf{k}_1|^2 = \left(\frac{4\pi}{\lambda_0}\right)^2 \left\{ n_k^2(2\omega_0,\theta_2)\sin^2\alpha + \left[n_k(2\omega_0,\theta_2)\cos\alpha - \frac{1}{2} n_i(\omega_0,\theta_0) \right]^2 \right\}. \tag{21}$$

But $|\mathbf{k}_1|^2$ can also be written

$$|\mathbf{k}_1|^2 = \left(\frac{2\pi}{\lambda_0}\right)^2 n_j^2(\omega_0,\theta_1), \tag{22}$$

where θ_1, the angle between $\mathbf{k}_1$ and the c axis, satisfies the equation

$$\cos\theta_1 = \frac{\mathbf{k}_1 \cdot \hat{c}}{|\mathbf{k}_1| \cdot |\hat{c}|} \tag{23}$$

$$= \cos\theta_0 + \frac{n_k(2\omega_0,\theta_0)\sin\theta_0}{n_k(2\omega_0,\theta_0) - \frac{1}{2} n_i(\omega_0,\theta_0)} \alpha\cos\beta - \frac{2A_2 n_i(\omega_0,\theta_0)\sin\theta_0}{[2n_k(2\omega_0,\theta_0) - n_i(\omega_0,\theta_0)]^2} \alpha^2\cos^2\beta - \frac{2n_k^2(2\omega_0,\theta_0)\cos\theta_0}{[2n_k(2\omega_0,\theta_0) - n_i(\omega_0,\theta_0)]^2} \alpha^2 \tag{24}$$

Setting the two expressions for $|\mathbf{k}_1|^2$ equal, we obtain an exact expression that holds for any SHG process, type I or II:

$$4n_k^2(2\omega_0,\theta_2) + n_i^2(\omega_0,\theta_0) - 4n_i(\omega_0,\theta_0)n_k(2\omega_0,\theta_2)\cos\alpha = n_j^2(\omega_0,\theta_1). \tag{25}$$

Equation (25) along with Eqs. (6), (9), and (24) yields an exact implicit function for the locus of phase-matched second-harmonic $\mathbf{k}$ vectors in terms of the angular polar coordinates α and β.

Working to second order in α, we find using Eqs. (6) and (9)

$$n_k(2\omega_0,\theta_2) = n_k(2\omega_0,\theta_0) + A_2\alpha\cos\beta + \frac{1}{2}B_2\alpha^2\cos^2\beta + \frac{1}{2}C_2\alpha^2, \tag{26}$$

where A_2 is given by Eq. (13) and

$$B_2 = b_2 n_e^3(2\omega_0,\theta_0)\sin^2\theta_0[1 + 3b_2 n_e^2(2\omega_0,\theta_0)\cos^2\theta_0], \tag{27}$$

$$C_2 = -b_2 n_e^3(2\omega_0,\theta_0)\cos^2\theta_0, \tag{28}$$

if $k = e$. Otherwise, $A_2 = B_2 = C_2 = 0$, as before. Similarly,

$$n_j^2(\omega_0,\theta_1) \approx n_j^2(\omega_0,\theta_0) + \tilde{A}_1\alpha\cos\beta + \tilde{B}_1\alpha^2\cos^2\beta + \tilde{C}_1\alpha^2, \tag{29}$$

where

$$\tilde{A}_1 = 2b_1\frac{n_k(2\omega_0,\theta_0)n_e^4(\omega_0,\theta_0)}{2n_k(2\omega_0,\theta_0) - n_i(\omega_0,\theta_0)}\sin 2\theta_0 \tag{30}$$

$$= 4\frac{n_k(2\omega_0,\theta_0)n_e(\omega_0,\theta_0)}{2n_k(2\omega_0,\theta_0) - n_i(\omega_0,\theta_0)}A_1 \tag{31}$$

$$\tilde{B}_1 = 4b_1\frac{n_k^2(2\omega_0,\theta_0)n_e^4(\omega_0,\theta_0)}{[2n_k(2\omega_0,\theta_0) - n_i(\omega_0,\theta_0)]^2}\sin^2\theta_0 + 4b_1^2\frac{n_k^2(2\omega_0,\theta_0)n_e^6(\omega_0,\theta_0)}{[2n_k(2\omega_0,\theta_0) - n_i(\omega_0,\theta_0)]^2}\sin^2 2\theta_0 - 2b_1A_2\frac{n_i(\omega_0,\theta_0)n_e^4(\omega_0,\theta_0)}{[2n_k(2\omega_0,\theta_0) - n_i(\omega_0,\theta_0)]^2}\sin 2\theta_0 \tag{32}$$

$$\tilde{C}_1 = -4b_2\frac{n_k^2(2\omega_0,\theta_0)n_e^4(\omega_0,\theta_0)}{[2n_k(2\omega_0,\theta_0) - n_i(\omega_0,\theta_0)]^2}\cos^2\theta_0 \tag{33}$$

if $j = e$. If $j = 0$, then $\tilde{A}_1 = \tilde{B}_1 = \tilde{C}_1 = 0$. Note that this expansion does not reduce exactly in the first order to Eq. (10). This is because the small birefringence approximation made in Eq. (7) is not made in the more precise expression represented by Eqs. (29)–(33). It should also be mentioned that significant simplification in these expressions can result if terms second order and higher in the birefringence parameters b_1 and b_2 are dropped; most applications should allow this simplification especially when $\theta \approx 90°$.

Substitution of Eqs. (26) and (29) into Eq. (25) results in the equation

$$U\alpha^2 + V\alpha^2\cos^2\beta - 2W\alpha\cos\beta + X = 0, \tag{34}$$

where

$$U = 2n_i(\omega_0,\theta_0)n_k(2\omega_0,\theta_0) - 2C_2n_i(\omega_0,\theta_0) + 4C_2n_k(2\omega_0,\theta_0) - \tilde{C}_1, \tag{35}$$

$$V = 4A_2^2 + 4B_2n_k(2\omega_0,\theta_0) - 2B_2n_i(\omega_0,\theta_0) - \tilde{B}_1, \tag{36}$$

$$W = 2A_2n_i(\omega_0,\theta_0) - 4A_2n_k(2\omega_0,\theta_0) + \frac{1}{2}\tilde{A}_1, \tag{37}$$

$$X = [2n_k(2\omega_0,\theta_0) - n_i(\omega_0,\theta_0)]^2 - n_j^2(\omega_0,\theta_0). \tag{38}$$

Equation (34) is the equation of an elliptical cone of rays giving rise to an elliptical pattern at the exit face of the crystal with center coordinate α_c and semimajor axes α_x and α_y, where

$$\alpha_c = \left(\frac{W}{U+V}\right), \tag{39}$$

$$\alpha_x^2 = \left(\frac{1}{U+V}\right)\left(\frac{W^2}{U+V} - X\right), \tag{40}$$

$$\alpha_y^2 = \left(\frac{1}{U}\right)\left(\frac{W^2}{U+V} - X\right). \tag{41}$$

The problem of displacement due to Poynting vector walkoff can be treated by noting that the second-harmonic radiation created just before the exit face of the crystal will experience negligible displacement. Thus measurement of the elliptical ring parameters should be performed with as thin a beam as possible looking only at the rightmost (or leftmost depending on the direction of the walkoff) edge of the pattern.

Any practical arrangement for angle measurement in this technique will involve observing the patterns on a distant viewing screen and taking into account the effect of refraction at the exit face of the crystal. Different crystal cuts will of course affect the patterns differently, and it is suggested that a vidicon array in combination with a computer be used for maximum ease and precision in determining ring parameters. In view of the complexity of the expressions for these parameters and the possibility of obtaining statistical data using many values of the crystal tilt angle, a computer curve-fitting program at the very least is required to extract the parameters of interest from the measured quantities.

VI. Application to SHG Optimization

An additional application of these rings is to the optimization of SHG by hand or by machine. Because the rings have known radii and are tangent to the main beam spot when the collinear phase-matching condition is achieved, their size and/or position could be monitored and a signal fed back to the crystal mount positioners or oven to maintain maximum SHG. The advantage of such a technique is that no additional optics need be placed in the usually intense main beam, thus precluding (1) the possibility of damage to such optics, (2) phase front distortion in the second-harmonic beam by the aforementioned optics, and (3) any loss in second-harmonic intensity. It is possible, however, that scattering of the intense phase-matched second-harmonic may obscure the relatively weak ring(s). Use of this optimization method would be facilitated by orienting the crystal with its higher quality regions near the exit face (rather than the entrance face) to minimize this scattering.

The author would like to thank Anthony E. Siegman and Robert L. Byer for their suggestions and encouragement and also Jean-Marc Heritier for helpful discussions. The photographic assistance of David Ziony was also greatly appreciated. Last, the author wishes to thank the referee for providing the reference to J. A. Giordmaine's original work on the subject, of which the author was unaware. This work was supported by the Joint Services Electronics Program.

References

1. P. D. Maker, R. W. Terhune, M. Nisenoff, and C. M. Savage, Phys. Rev. Lett. 8, 21 (1962).
2. D. A. Kleinman, A. Ashkin, and G. D. Boyd, Phys. Rev. **145**, 338 (1966).
3. J. A. Giordmaine, Phys. Rev. Lett. 8, 19 (1962).
4. R. A. Baumgartner and R. L. Byer, IEEE J. Quantum Electron. **QE-15**, 432 (1979).